RSC Advances

This article can be cited before page numbers have been issued, to do this please use: V. Verdinelli, A. Juan, J. M. Marchetti and E. German, *RSC Adv.*, 2016, DOI: 10.1039/C6RA12964A.

ROYAL SOCIETY OF CHEMISTRY

www.rsc.org/advances

View Article Online
DOI: 10.1039/C6RA12964A

A MICROSCOPIC LEVEL INSIGHT INTO Pt DOPED TiZn (001) SURFACE FOR HYDROGEN ENERGY STORAGE USAGE

V.Verdinelli[a*], A. Juan[b], J.M. Marchetti[c], E. Germán[b]

[a] *IFISUR, Universidad Nacional del Sur, CONICET, Departamento de Química - UNS, Av. L. N. Alem 1253, B8000CPB - Bahía Blanca, Argentina.*
[b] *IFISUR, Universidad Nacional del Sur, CONICET, Departamento de Física - UNS, Av. L. N. Alem 1253, B8000CPB - Bahía Blanca, Argentina.*
[c] *Department of Mathematical Science and Technology, Norwegian University of Life Sciences, Drøbakveien 31, Ås, 1432, Norway.*

[*] *corresponding author*
Dr. Valeria Verdinelli
Departamento de Química & Instituto de Física del Sur
Universidad Nacional del Sur-CONICET
Av. Alem 1253
(8000) Bahía Blanca
Argentina
vverdinelli@uns.edu.ar
Tel: +54-9-291-4882982 Int.: 33
Fax: +54-9-291-4595142

View Article Online
DOI: 10.1039/C6RA12964A

ABSTRACT

The interaction of hydrogen and platinum with B2-TiZn (001) surface was studied by means of spin-polarized density functional theory (DFT) calculations. H and Pt on TiZn adsorption energies were calculated taking into account high symmetry adsorption sites. Both adatoms prefer to be adsorbed on the hollow site where the higher coordination number allows them to minimize the repulsion among the overlapping charge densities of them and surface. Furthermore, the influence of pre-adsorbed Pt on the H adsorption was analyzed in detail. It was found that this process is enhanced when Pt is doping TiZn surface. The electronic structures and changes in the chemical bonding for both adsorbates on Ti alloy surface were computed by density of states (DOS) and overlap population (OP) methods, concluding that $3d_{x^2-y^2}$, $3d_{z^2}$ and $3p_z$ Ti, $5p_z$ Pt orbitals play an important role in H adsorption, as well as it was deduced that the strong overlap between Pt and Ti orbitals allows H atoms bond more effectively on the surface. A Bader's analysis revealed that H and Pt act as electron acceptors while surface Ti atoms act as electron donors during the H adsorption process.

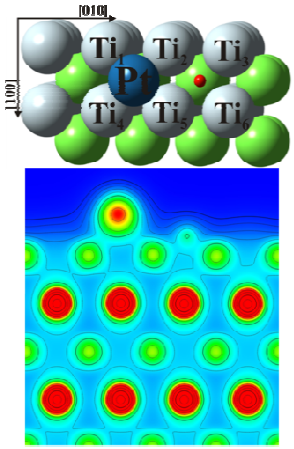

H-storage behavior on TiZn and Pt-doped TiZn alloys

View Article Online
DOI: 10.1039/C6RA12964A

1. INTRODUCTION

Energy is considered a key input for a sustainable development. Among of the potential solutions to the current environmental problems hydrogen and fuel cell energy systems appear to be the most effective ones. Also, they can play a significant role in providing not only a better environment and sustainability but also a clean, safe, reliable and secure energy supply[1]. Nevertheless, hydrogen storage is a challenge because it implies the reduction of a huge volume of hydrogen gas as well as the reversibility of uptake and release[2].

Moreover, the hydrogen adsorption study in materials plays a crucial role in the material science. In many metals, it can lead to premature failure under stress, a phenomena referred as hydrogen embrittlement. This mechanism is believed to be different depending on whether or not stable hydrides can be formed. Metal hydrides are also important as a potential hydrogen source for small portable fuel cells[3]. Reversible hydriding can be used as a fuel storage mechanism for operation with large fuel cells for stand-alone power or for automobiles [4-7].

Many researchers have investigated hydrogen adsorption, dissociation and diffusion on metallic surfaces[8-10], being Mg-based metal hydrides one of the most studied for competitive mobile hydride storage with the reversible hydrogen capacity of up to 7.6 wt%[11]. Unfortunately, the main disadvantages of MgH_2 as a hydrogen store are slow desorption kinetics, the high temperature of hydrogen discharge, and a high reactivity toward air and oxygen[12,13].

Besides a variety of materials such as $LaNi_5$, FeTi, AB_2 type compounds and Ti-based body centered cubic (BCC) alloys are well known as systems with potential

View Article Online
DOI: 10.1039/C6RA12964A

hydrogen storage applications[2-6, 14]. Although these materials are attractive for their operational safety, high volumetric density and low energy inputs; they present a critical drawback: their low gravimetric energy density at ambient temperature and pressure[15].

Among AB-type intermetallic materials, TiZn systems have gained importance in recent years for their many practical applications[16-20]. TiZn compounds play a significant role in the galvanizing steel industry[21-24] and they are used as metal coatings for corrosion protection[25,26]. However there is still a lot of aspects to study regarding H-storage behavior in these alloys.

On the other side, Platinum (Pt) is one of the most practical catalysts because of its excellent activity and durability[27]. Although Pt has major environmental applications in technological important areas, such as the catalytic conversion of biomass to hydrogen, it is an extremely expensive and natural limited resource[28]. Because of this, it is desirable to develop new catalysts with reduced Pt content and good performance[29].

The hydrogen interaction with TiZn (001) surface and Pt-doped TiZn surface was studied. The preferential adsorption geometries, adsorption energies and electronic properties were determined using spin-polarized density functional theory (DFT) calculations. The concept of density of states (DOS), overlap population (OP) and Bader charge were employed in the analysis of electronic structure and bonding evolution.

View Article Online
DOI: 10.1039/C6RA12964A

2. THEORETICAL METHOD AND ADSORPTION MODEL

Spin-polarized density functional theory (DFT) calculations were performed[30] using the Vienna Ab initio Simulation Package (VASP)[31]. The projector-augmented wave (PAW) pseudopotencial[32,33] was used to account for the electron-ion core interaction, using the Perdew-Burke-Ernzerhof form of the generalized gradient approximation (GGA-PBE)[34] for exchange-correlation term.

The TiZn (001) surface was simulated using a (2 x 4) slab model containing 24 Ti and 16 Zn atoms and a 21 Å vacuum in the [001] direction (see Figure 1(a)). The Brillouin zone was integrated using an 11 x 11 x 1 Monkhorst-Pack *k*-point mesh[35]. For the plane-wave basis set a cutoff of 500 eV was used. Both selected values were optimized searching for convergence for the sake of balance between calculation time and accuracy. The top three layers of the slab were relaxed while the bottom two layers were kept fixed to the bulk positions in order to minimize the computational cost. The total energy convergence and the forces on the atoms were less than 10^{-5} and 0.01eV/Å, respectively. Self-consistent calculations were considered to converge when the difference in surface total energy between consecutive steps did not exceed 10^{-6} eV. In the same way, static calculations were considered to converge using the same criterion.

To understand hydrogen-metal and metal-metal interactions and bonding we used the concepts of density of states (DOS) and atom projected density of states (PDOS). The last was calculated by projecting one-electron states onto spherical harmonic atomic orbitals centered on atomic sites. A qualitative study of the bonding between different atoms was also performed using the overlap population (OP) concept in extended structures (OPDOS)[36,37], as implemented in the SIESTA code[38,39]. The same approach was recently

View Article Online
DOI: 10.1039/C6RA12964A

used to analyze the changes in bonding after adsorption in Pt and VSb mixed oxydes[40,41] and others systems[42-44]. Additional bonding analysis was calculated by the DDEC6 method[45-47]. Bader analysis[48] as implemented by Tang et al.[49] was used to calculate electronic charges on atoms.

The calculated lattice parameter obtained for bulk TiZn, which crystallizes in a CsCl structure ($Pm\bar{3}m$, group N°221), was a_0 = 3.141 Å, which is in good agreement with the experimental value (a_0 = 3.146 Å)[50] and theoretical value a_0 = 3.138 Å[18]. The TiZn surface was computed using the obtained bulk parameter. We considered high-symmetry sites for H and Pt adsorption on the Ti alloy i.e. on top of Ti atom (T_s), in a bridge between two nearest-neighbor surface atoms (B_s) and in a hollow site (H_s) (Figure 1).

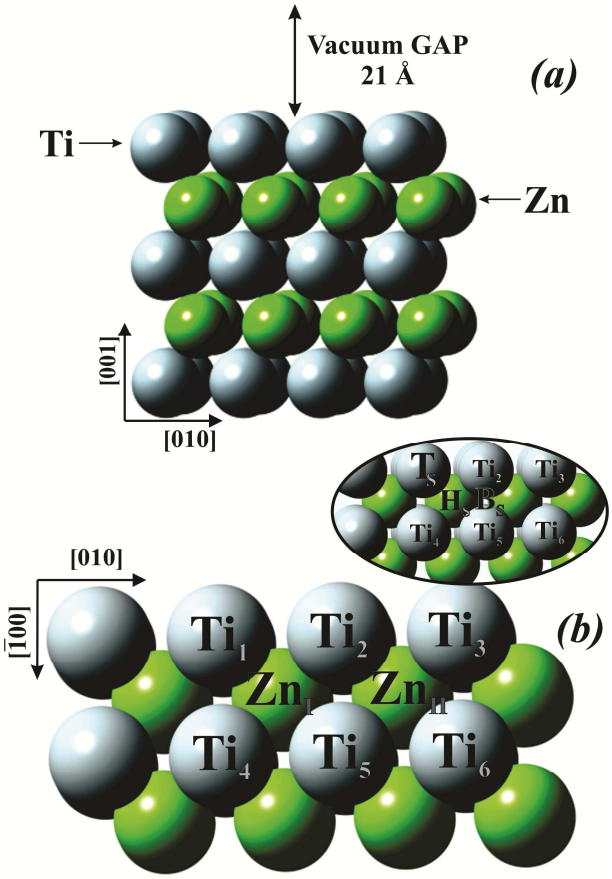

Figure 1. (a) Side view of TiZn (001) slab model (b) schematic top view of slab model and location of the studied adsorption sites.

View Article Online
DOI: 10.1039/C6RA12964A

First, we considered the adsorption energy of a Pt atom on TiZn surface, following the equation:

$$E_{ads}\,(Pt) = E_{(Pt\,/\,TiZn)} - E_{(Pt)} - E_{(TiZn)} \quad (1)$$

where $E_{(Pt/TiZn)}$ is the total energy of the adatom Pt adsorbed on TiZn surface, $E_{(TiZn)}$ is the energy of the pure TiZn surface and $E_{(Pt)}$ is the energy of an isolated Pt in a cubic box of 10 x 10 x 10 $Å^3$.

The binding (E_b) and adsorption (E_{ads}) energies for hydrogen addition on TiZn and Pt/TiZn were calculated according to the following expression given by Lee et al.[51].

$$E_b\,(H) = E_{(H\text{-}S)} - E_{(S)} - E_{(H)} \quad (2)$$

$$E_{ads}\,(H) = E_{(H\text{-}S)} - E_{(S)} - \tfrac{1}{2}\,E_{(H2)} \quad (3)$$

where $E_{(H)}$ is the energy of one H atom and $E_{(H2)}$ is the energy of one isolated H_2 molecule in a cubic box of 10 x 10 x 10 $Å^3$. H-H bond length of 0.750 Å and a binding energy of -4.538 eV were found in fairly good agreement with experimental values[52] and theoretical calculations[53]. $E_{(H\text{-}S)}$ is the total energy of the H adsorbed on the surface; $E_{(S)}$ is the energy of the pure TiZn surface. It should be noted that when H is considered on Pt doped TiZn, $E_{(H\text{-}S)}$ is the total energy of the H adsorbed on Pt/TiZn surface and $E_{(S)}$ is the energy of the Pt adsorbed on TiZn (001) surface.

View Article Online
DOI: 10.1039/C6RA12964A

3. RESULTS AND DISCUSSIONS

3.1 Hydrogen and Platinum adsorption on TiZn (001) surface

Spin-polarized calculations were carried out in order to get the optimal electronic structure and valid energy values. We obtained a magnetism of 3.187 μB for the bare surface. Transition metal (TM) elements are known for presenting effects due to their *d*-electrons, i.e. relatively strong localization (inducing magnetic moments, formed mainly because of the intra-atomic exchange interaction), directional bonding and high density of states near the Fermi level[54].

The total and Ti- and Zn- projected density of states (DOS and PDOS) curves for the bare surface are shown in Figure 2. It can be noticed that Ti and Zn states are strongly hybridized between -8.5 eV and 3 eV. These results are in agreement with theoretical calculations reported by Gosh et al.[18] who also reported strong hybridization effects between Zn and Ti atoms.

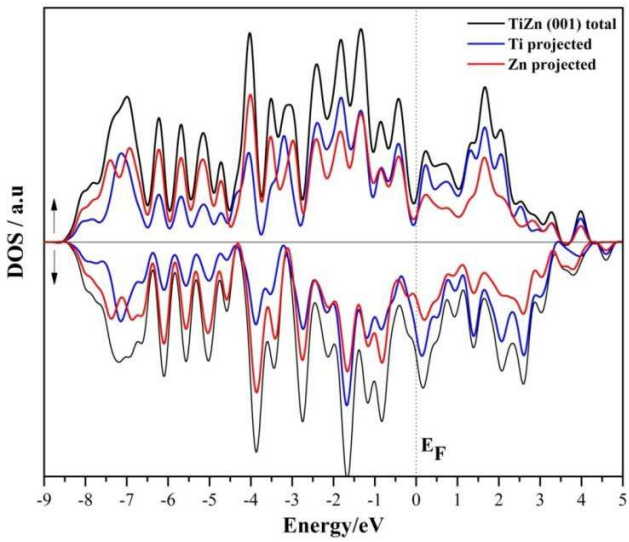

Figure 2. DOS (in black) and PDOS curves for pure TiZn (001) surface calculated by VASP. The PDOS for Ti and Zn are plotted using blue and red lines, respectively.

View Article Online
DOI: 10.1039/C6RA12964A

The adsorption of Pt and H on TiZn was studied taking into account the three sites previously described. It was found that the H_S site is the most favorable for H and Pt adsorption on the surface (see Figures 1 and 3 and Table 1). Similar results were reported for other (001) surfaces[55,56].

Table 1. H and Pt binding energies, E_b (eV), for all studied systems

Site	H-TiZn	Pt-TiZn	H-Pt/TiZn
T_s	-0.078	-3.087	-2.479
B_s^*	$B_s \rightarrow H_s$	$B_s \rightarrow H_s$	$B_s \rightarrow H_s$
H_s	-1.092	-5.208	-3.141
Top Pt	-	-	-2.205

*After relaxation, Pt and H atoms which were located originally in B_s site move to H_s (Bs→Hs)

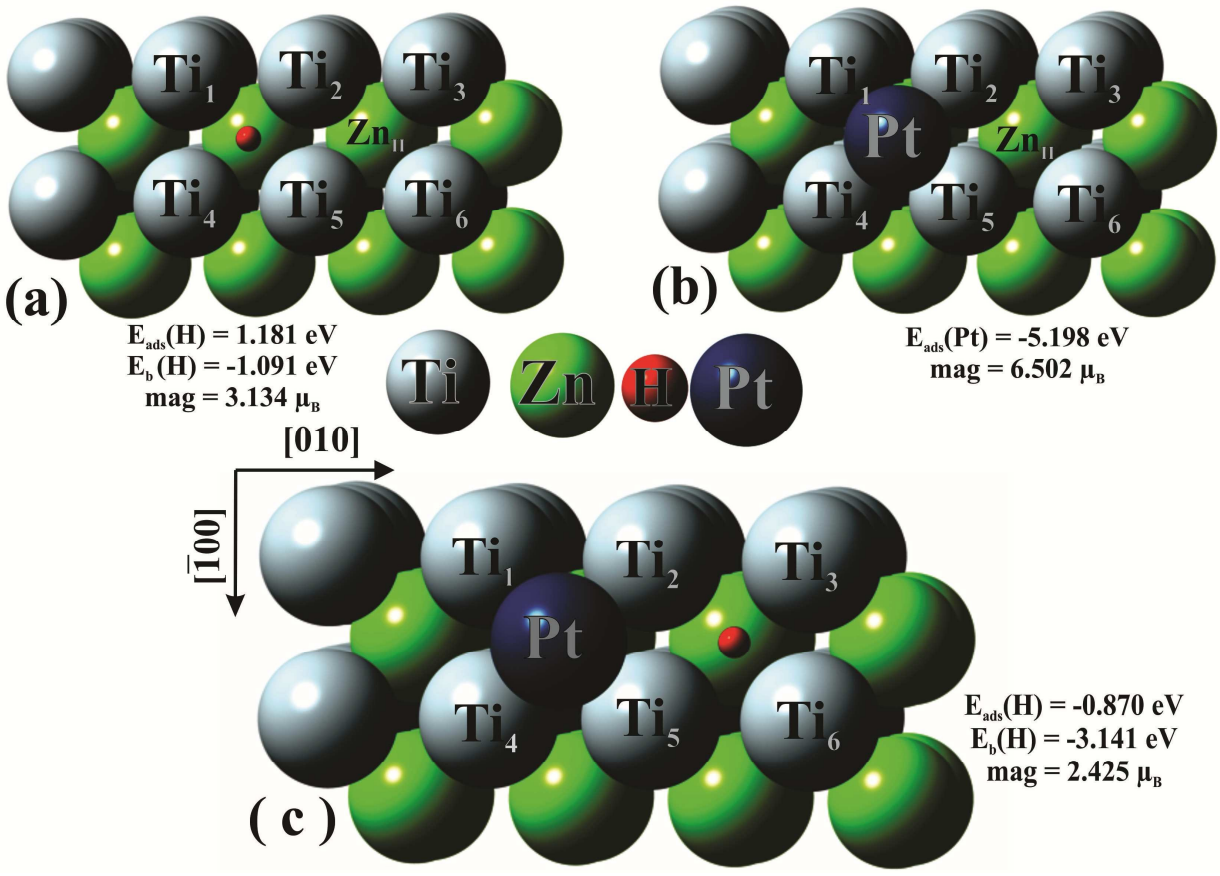

Figure 3. Schematic top view of TiZn (001) surface and the adsorption sites: (a) H adsorption and (b) Pt adsorption on TiZn and (c) H adsorption on Pt-TiZn

View Article Online
DOI: 10.1039/C6RA12964A

The optimized bond lengths and OP values for the clean TiZn surface, H-TiZn and Pt-TiZn are presented in Table 2. The calculated binding energy of H atom on pristine TiZn (001) was -1.091 eV at a H-Ti distance of 2.122 Å with an OP value of 0.152, as H atom is located on a hollow site it interacts equally with 4 Ti atoms namely Ti_1, Ti_2, Ti_4 and Ti_5 in Figure 1, with a total overlap of 0.606. Kulkov et al.[55] reported a H-Ti distance of 1.86-1.92 Å for metal-terminated surface Me/TiMe (001) and Gupta et al.[57] computed a H-Ti distance of 2.189 Å for TiNiH compound; our results are in fair agreement with these calculations.

Meanwhile, Pt adsorption energy calculated according eq. 1 was -5.198 eV. Ti-Pt bonds are originated with lengths and OP values between 2.574-2.577 Å and 0.705-0.712, respectively, as Pt atom is also located on a Hs, it interacts with 4 Ti atoms giving a total overlap of 2.836. This is a strong bond between Pt and the surface, inasmuch as only TMs are involved. Similar findings were computed by Celik et al.[58] for Pt/TiO_2 where the authors found a Pt-Ti bond length of 2.49 Å. In both cases, H and Pt adsorption processes almost no H-Zn or Pt-Zn interaction was detected.

It can be seen in Table 2 that OP values decrease for Ti-Ti bonds near to the adsorption sites by 23% while OP for Ti-Zn bonds diminish by 2% when Ti-H bonds are formed. Meanwhile, OP values for Ti-Ti bonds and Ti-Zn bonds show a reduction by 50% and 11% respectively, after Pt adsorption. These results indicate that the interaction between Pt and Ti are stronger than H and Ti. On the other side, Zn-Zn bonds are slightly affected. A similar analysis can be done using OPs computed with DDEC6[45,46] from VASP output files. Table 2 presents the values for selected bonds. Although a direct comparison of absolute values with those from SIESTA cannot be done, the changes and the tendency of decreasing or increasing in a particular OP present a similar behavior.

View Article Online
DOI: 10.1039/C6RA12964A

Table 2. Bond distances (d) and Overlap Population (OP) for optimized TiZn surface, H-TiZn and Pt-TiZn[a] systems

Bond	TiZn (001)		H-TiZn (001)			Pt-TiZn (001)	
	d/Å	OP (SIESTA)	d/Å	OP (SIESTA)	OP[b] (DDEC6)	d/Å	OP (SIESTA)
Ti_1-Ti_2	2.706	0.435	2.683	0.351	0.314	2.730	0.219
Ti_2-Ti_3	2.706	0.435	2.698	0.446	0.370	2.690	0.400
Ti_2-Ti_5	2.706	0.427	2.693	0.331	0.307	2.748	0.219
Ti_4-Ti_5	2.706	0.435	2.684	0.351	0.314	2.728	0.221
Ti_5-Ti_6	2.706	0.435	2.698	0.450	0.370	2.689	0.402
Zn_I-Zn_{II}	2.706	0.205	2.700	0.210	0.268	2.683	0.221
Ti_1-Zn_I	2.771	0.223	2.771	0.218	0.225	2.795	0.203
Ti_2-Zn_I	2.771	0.224	2.771	0.219	0.225	2.805	0.198
Ti_4-Zn_I	2.771	0.224	2.771	0.219	0.225	2.805	0.198
Ti_5-Zn_I	2.771	0.223	2.771	0.218	0.225	2.799	0.201
H-Ti_1			2.122	0.151	0.224		
H-Ti_2			2.122	0.152	0.224		
H-Ti_4			2.122	0.152	0.224		
H-Ti_5			2.122	0.151	0.223		
H-Zn_I			2.960	0.009	0.028		
Pt-Ti_1						2.574	0.708
Pt-Ti_2						2.576	0.712
Pt-Ti_4						2.577	0.711
Pt-Ti_5						2.577	0.705
Pt-Zn_I						3.724	0.007

[a] See atom labeling in Fig. 1(b) and Fig. 3.
[b] OP computed with DDEC6 for selected bonds[47]

It can be seen in Table 3 that the binding in the hollow position occurs mainly through the combination of H 1s and Ti 4s, $3d_{xy}$ and $3d_{xz}$ states in the case of hydrogen adsorption, whereas Pt atom suffers a rearrangement of its orbital occupation during the bonding process and interacts mainly with $3p_z$, $3d_z^2$ and $3d_{x^2-y^2}$orbitals of surface Ti atoms. Similar results were reported by Lee et al.[51]. On the other hand, electron orbital occupations of Zn remain without meaningful changes during both adsorption processes.

View Article Online
DOI: 10.1039/C6RA12964A

Table 3. Electron Orbital Occupations for Optimized TiZn surface, H-TiZn and Pt-TiZn systems (VASP)

	s	p_x	p_y	p_z	$d_{x^2-y^2}$	d_{z^2}	d_{xy}	d_{xz}	d_{yz}
Bare atom									
Pt	0.00	0.00	0.00	0.00	2.00	2.00	2.00	2.00	2.00
H	1.00	0.00	0.00	0.00	0.00	0.00	0.00	0.00	0.00
$TiZn_{surface}$									
Ti	0.69	0.06	0.06	0.06	0.77	0.33	0.57	0.54	0.54
Zn	1.19	0.45	0.46	0.52	1.99	1.99	1.99	1.99	1.99
H-TiZn									
H	1.54	0.00	0.00	0.00	0.00	0.00	0.00	0.00	0.00
Ti	0.61	0.06	0.06	0.06	0.80	0.32	0.50	0.51	0.53
Zn	1.19	0.45	0.46	0.51	1.99	1.99	1.99	1.99	1.99
Pt-TiZn									
Pt	1.52	1.36	1.36	1.50	1.92	1.93	1.90	1.93	1.93
Ti	0.61	0.07	0.07	0.12	0.49	0.39	0.48	0.46	0.49
Zn	1.20	0.44	0.45	0.49	1.99	1.99	1.99	1.99	1.99

Regarding the Ti-H, Pt-Ti, Ti-Ti and Zn-Zn OPDOS curves, it can be observed that the interactions are mainly bonding, Figure 4 (a)-(f). As a reference, contributions above the horizontal axis are bonding between specified atoms, while contributions below are antibonding. Figure 4 (a) and (d) show a strong overlapping among H and Ti atoms and among Pt and Ti atoms, respectively. When H atom is adsorbed on TiZn surface, the bonding area of Ti-Ti bonds decreases while the bonding area of Zn-Zn bonds is not affected (see Figure 4 (b) and (c)). A similar behavior is found when Pt atom is adsorbed on the (001) surface (see Figure 4 (e) and (f)). Also it can be observed that Ti-Zn OPDOS curves do not show significant changes after H or Pt adsorption.

View Article Online
DOI: 10.1039/C6RA12964A

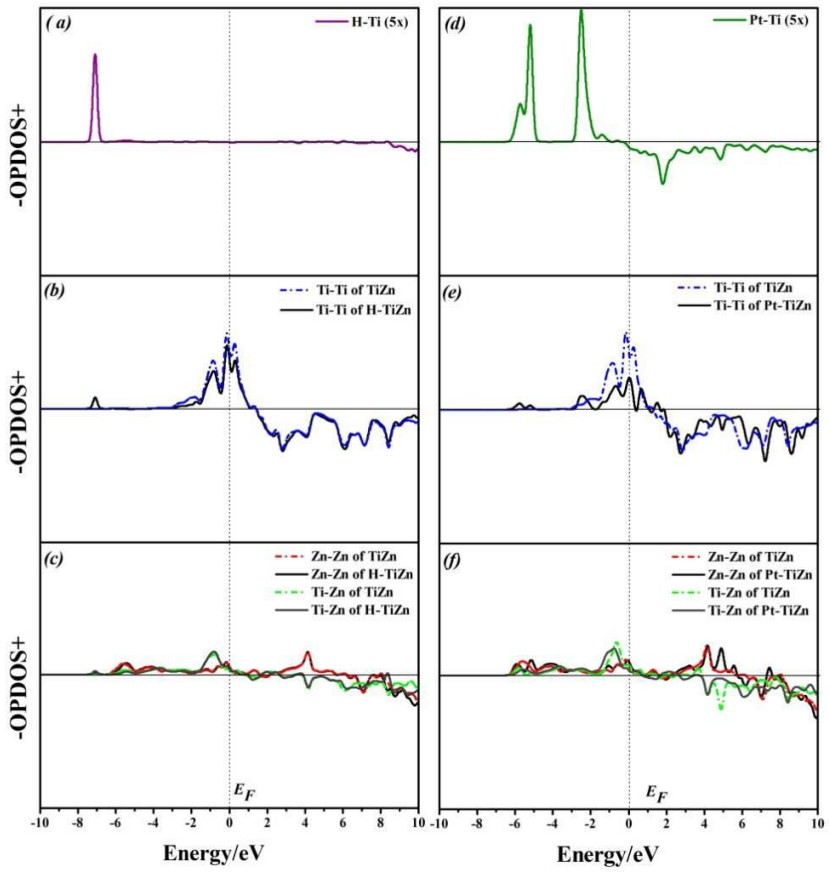

Figure 4. OPDOS curves of selected bonds: (a) H-Ti formed bond, (b) Ti-Ti bonds before and after, (c) Zn-Zn and Ti-Zn bonds before and after H adsorption on TiZn, (d) Pt-Ti formed bond, (e) Ti-Ti bonds before and after, (f) Zn-Zn and Ti-Zn bonds before and after Pt adsorption on TiZn. All calculations from SIESTA.

The DOS curves corresponding to H-TiZn and Pt-TiZn are plotted in Figure 5 from panel (a) to panel (f). It can be observed that systems maintain the strong states hybridization after H or Pt adsorption on TiZn, mainly near the Fermi level. Moreover, H band states are stabilized at -5 eV below the E_F whereas the main Pt band states are located between -4.8 eV and -1.80 eV. In both cases, Zn and Ti states are mixed in all plotted energy range.

View Article Online
DOI: 10.1039/C6RA12964A

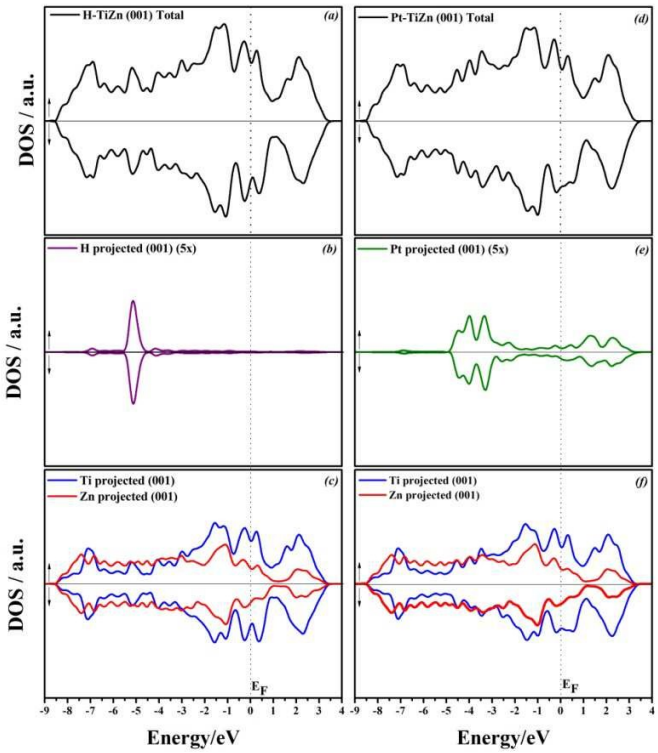

Figure 5. DOS curves for: (a) H-TiZn total, (b) H atom projected, (c) Ti atoms and Zn atoms projected corresponding to H-TiZn, (d) Pt-TiZn total, (e) Pt atom projected, (f) Ti atoms and Zn atoms projected corresponding to Pt-TiZn as calculated by VASP.

Also, it can be observed that H adsorption on TiZn surface leads to a slightly decrease in the magnetic moment from 3.187 μB (clean surface) to 3.134 μB (H-TiZn). In contrast, Pt adsorption increases the total magnetic moment from 3.187 μB to 6.502 μB (Pt-TiZn) which is expected from the unfilled *d* shell of TMs.

3.2 Hydrogen adsorption on Pt/TiZn (001)

When a hydrogen atom is adsorbed on Pt-doped TiZn, it is also located on a H_s position with Ti-H bond distances between 2.056 and 2.148 Å and Zn-H bond distance of 2.902 Å. The H adsorption energy is enhanced from 1.181 eV (on TiZn) to -0.870 eV on Pt-TiZn, the negative value indicates that no energy is required in order to adsorb a H atom

View Article Online
DOI: 10.1039/C6RA12964A

on the surface. The H binding energy is improved as well from -1.091 eV (on TiZn) to -3.141 eV on Pt-TiZn, the last value is similar to those obtained by Kulkova et al[59] in which authors have studied the binding energy of H atom on some pure and TM doped-titanium alloy (001) surfaces, their values are around -2.62 and -3.25 eV depending on which atom H is bonded to. Most of the articles in literature report H_2 binding energy which cannot be used to compare our results. However, Jeloaica et al.[60] have reported the binding energy for H atom on graphene, obtaining an energy of about -0.57 eV. Recently, Zhuang et al.[61] have calculated the hydrogen binding energy for an H atom on Tungsten carbide (WC) pure and Pt doped; they have found that hydrogen binding energies for the W- and C-terminated are as large as -0.98 to -1.17 eV when the H atoms are adsorbed on the most stable sites, respectively. We can see that the presence of TMs improves the interaction of H with the surface. Moreover, H introduces a decrease in the total magnetic moment of Pt-TiZn (001) system.

The OP values and bond distances corresponding to the adsorption process are presented in Table 4. In comparison with H-Ti bond lengths presented in Table 3, these results show that H-Ti_2 and H-Ti_5 bond lengths elongate 2% while their strength decreases by 24% ; in contrast, H-Ti_3 and H-Ti_6 strength is increased by 25%. At the same time, it can be seen that the OP values of Pt-Ti_1 and Pt-Ti_4 bonds are incremented by 6% whereas Pt-Ti_2 and Pt-Ti_5 diminish their distances by 10%.

There is no Pt-H bonding after H adsorption on Pt-doped TiZn (001) surface as it can be observed in Table 4 and Figure 6 (a). Nevertheless an energetic improvement can be seen when the H adsorption occurs in presence of Pt, this can be explained considering the total overlapping values, i.e. taking into account that both Pt and H atoms are adsorbed on hollow sites surrounded by four Ti atoms. In order to understand the magnitude of the

View Article Online
DOI: 10.1039/C6RA12964A

bonding it is needed to consider the four OP values involved in the adsorption. In the case of H adsorbed on pristine TiZn surface the total OP (1H - 4Ti atoms) value is 0.606; however, when H is adsorbed on Pt doped TiZn surface this value increases to 0.611. On the contrary, a total OP value of 2.836 is found for Pt adsorbed on clean surface; meanwhile, in presence of H this OP value diminishes to 2.775. This leads us to suggest that, the preference for the hollow position is related to two factors: the higher coordination number in this site and the minimization of the repulsion among the overlapping charge densities.

Table 4. Bond distances (d) and Overlap Population (OP) for Optimized H-Pt/TiZn[a]

Bond	**H-Pt/TiZn (001)**		
	d/Å	OP (SIESTA)	ΔOP%[b]
Ti_1-Ti_2	2.756	0.208	-5.0
Ti_2-Ti_3	2.696	0.293	-26.8
Ti_2-Ti_5	2.703	0.192	-12.5
Ti_4-Ti_5	2.756	0.207	-6.4
Ti_5-Ti_6	2.696	0.293	-27.1
Zn_I-Zn_{II}	2.691	0.222	0.5
Ti_1-Zn_I	2.792	0.207	2.0
Ti_2-Zn_I	2.810	0.198	0.0
Ti_2-Zn_{II}	2.790	0.208	-7.6
Ti_3-Zn_{II}	2.777	0.219	-5.2
Ti_4-Zn_I	2.791	0.205	3.5
Ti_5-Zn_I	2.810	0.198	-1.5
Ti_5-Zn_{II}	2.790	0.205	-8.1
Ti_6-Zn_{II}	2.777	0.218	-5.2
H-Ti_2	2.148	0.115	-
H-Ti_3	2.056	0.190	-
H-Ti_5	2.148	0.117	-
H-Ti_6	2.056	0.189	-
H-Zn_{II}	2.902	0.010	-
Pt-H	3.060	0.000	-
Pt-Ti_1	2.542	0.751	6.1
Pt-Ti_2	2.639	0.636	-10.7
Pt-Ti_4	2.543	0.754	6.0
Pt-Ti_5	2.639	0.634	-10.1
Pt-Zn_I	3.749	0.008	0.0

[a] See atom labeling in Fig. 1(b) and Fig. 3

[b] Percentages are related to Pt atom adsorbed on surface

View Article Online
DOI: 10.1039/C6RA12964A

Moreover, Ti atoms participate in the bonding process mainly by their $3p_z$, $3d_{x-y}$ and $3d_{x^2-y^2}$ orbitals as we can see in Table 5. Also, it can be noticed that the bonding mechanism between Ti and Zn is still dominated by p-d hybridization.

Table 5. Electron Orbital Occupations for Optimized TiZn surface and H-Pt/TiZn system (VASP)

	s	**p_x**	**p_y**	**p_z**	**$d_{x^2-y^2}$**	**d_{z^2}**	**d_{xy}**	**d_{xz}**	**d_{yz}**
Bare atoms									
Pt	0.00	0.00	0.00	0.00	2.00	2.00	2.00	2.00	2.00
H	1.00	0.00	0.00	0.00	0.00	0.00	0.00	0.00	0.00
TiZn$_{clean\ surface}$									
Ti	0.69	0.06	0.06	0.06	0.77	0.33	0.57	0.54	0.54
Zn	1.19	0.45	0.46	0.52	1.99	1.99	1.99	1.99	1.99
H-Pt/TiZn									
H	1.53	0.00	0.00	0.00	0.00	0.00	0.00	0.00	0.00
Pt	1.52	1.36	1.36	1.50	1.93	1.93	1.90	1.93	1.93
Ti_2	0.56	0.06	0.07	0.10	0.49	0.35	0.42	0.46	0.48
Ti_3	0.61	0.05	0.05	0.06	0.71	0.28	0.51	0.49	0.54
Ti_4	0.61	0.06	0.07	0.12	0.45	0.39	0.50	0.46	0.47
Zn_I	1.20	0.43	0.45	0.49	1.99	1.99	1.99	1.99	1.99
Zn_{II}	1.20	0.45	0.45	0.51	1.99	1.99	1.99	1.99	1.99

The evolution of the chemical bonds was examined through the analysis of OPDOS curves for selected bonds (see Figure 6). As it can be noticed H-Ti, Pt-Ti, Ti-Ti and Zn-Zn interactions are mainly bonding after H adsorption on Pt/TiZn surface. While Pt-Ti (b) and Ti-Ti (c) bonds decrease their area under the E_F, Zn-Zn bonds (d) remain almost the same after H adsorption. In the case of H-Pt, bonding and antibonding areas are compensated, thus the interaction is non-bonding.

View Article Online
DOI: 10.1039/C6RA12964A

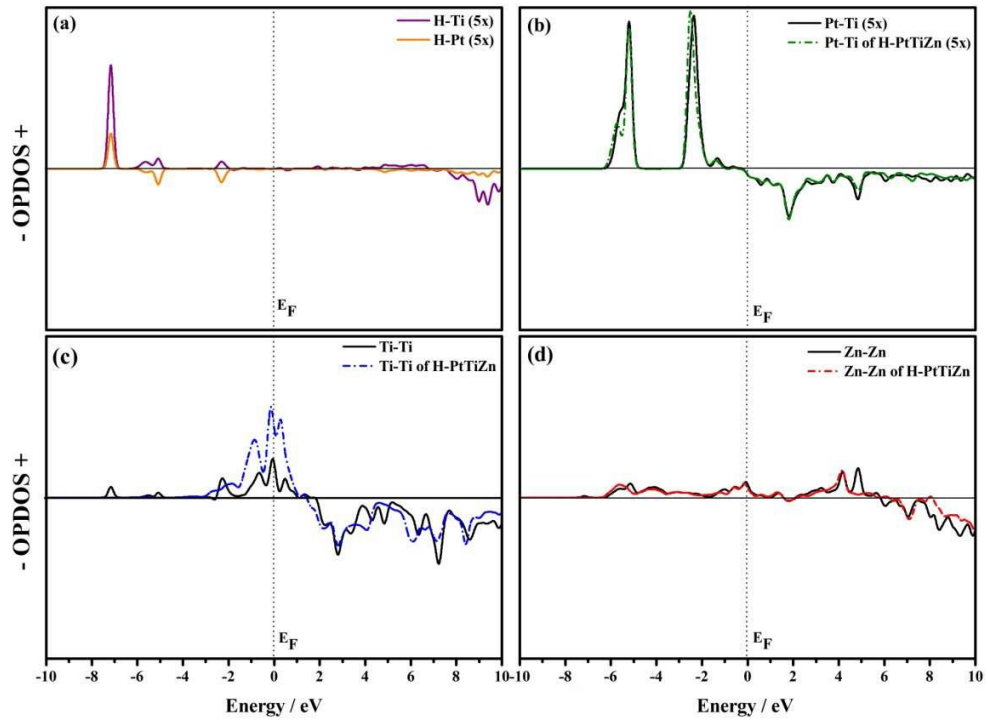

Figure 6. OPDOS curves for selected bonds: (a) H-Ti formed bond and H-Pt bond, (b) Pt-Ti bonds (c) Ti-Ti bonds and (d) Zn-Zn bonds before and after H adsorption on Pt/TiZn as calculated by SIESTA

The density of states (DOS) corresponding to H-Pt/TiZn is plotted in Figure 7 from panel (a) to panel (c). When H is adsorbed on Pt/TiZn, H 1s-state is located around -5.25 eV below E_F while Pt states are slightly displaced in comparison with those from Pt-TiZn without H, from -4.8 to -4.5 eV. Figure 7 (c) shows the Ti states and Zn states still strongly hybridized after H adsorption.

View Article Online
DOI: 10.1039/C6RA12964A

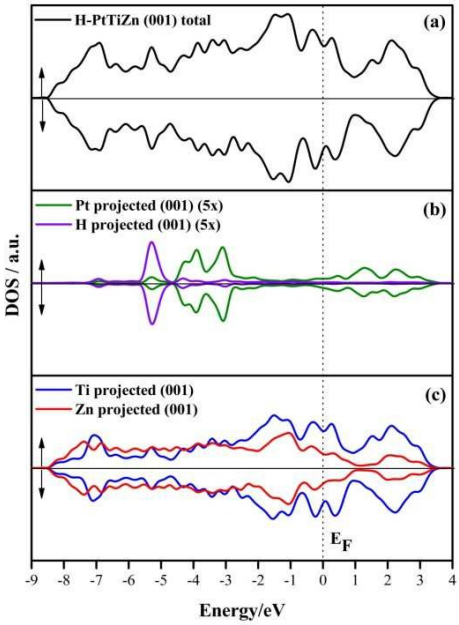

Figure 7. DOS curves for: (a) H-Pt/TiZn total, (b) H atom and Pt atom projected, (c) Ti atoms and Zn atoms projected corresponding to H-Pt/TiZn as calculated by VASP

3.3 CHARGE TRANSFER

As charge transfer is an important component in the nature of the surface metal-metal bonds[62] a Bader's analysis was performed[49].

In Table 6 the Bader's charges for all studied systems are presented. It can be noticed that Ti atoms act as electron donors; whereas Zn atoms act as electron acceptors given that Zn is more electronegative than Ti. This tendency can be seen in Figure 8 (a) which shows a contour plot of the charge density distribution for TiZn (001).

When H is adsorbed on the surface, it is surrounded by 4 Ti atoms which transfer a total charge of 0.431e^-. As a consequence of the charge transfer from Ti to H, Zn atoms diminish their electron density. Thus, Zn near to the adsorption site loses 0.103 e^-. In Figure 8 (b), it can be observed H charge density distribution in the H_s site and its interaction with

View Article Online
DOI: 10.1039/C6RA12964A

the nearest Ti atoms. A similar behavior was found in metal-transition hydrides reported by Smithson et al.[3].

Table 6. Bader's charge of TiZn (001), H-TiZn, Pt-TiZn, H-Pt/TiZn (in e^-) calculated by VASP

	TiZn (001)	***H-TiZn***	***Pt-TiZn***	***H-Pt/TiZn***
H		0.633		0.598
Pt			1.092	1.044
$\mathbf{Ti_1}$	-0.414	-0.536	-0.630	-0.625
$\mathbf{Ti_2}$	-0.414	-0.500	-0.633	-0.715
$\mathbf{Ti_3}$	-0.414	-0.333	-0.373	-0.543
$\mathbf{Ti_4}$	-0.414	-0.544	-0.634	-0.647
$\mathbf{Ti_5}$	-0.414	-0.507	-0.628	-0.738
$\mathbf{Ti_6}$	-0.414	-0.333	-0.423	-0.552
$\mathbf{Zn_I}$	0.788	0.685	0.678	0.650
$\mathbf{Zn_{II}}$	0.788	0.675	0.740	0.711

The contour map of charge density distribution of Pt-TiZn is shown in Figure 8 (c). A relatively high electron density region extends from the Pt atom site to the interacting Ti atom sites. As a result of the greater affinity among Pt and Ti atoms on the H_s site, the interaction among Zn and Ti is weakened. In this case, Ti atoms act as electron donors and lose between 0.214 and 0.220 e^- while Pt gains 1.092 e^- (see Table 6).

Finally, when H is adsorbed on Pt doped-TiZn, it can be noticed that H and Pt act as electron acceptors while Ti superficial atoms still act as electron donors. Since H and Pt are located in high-symmetry positions, they gain 0.598 e- and 1.044 e-, respectively whereas Zn atoms near the adsorption sites lose between 0.077 and 0.138 e- during the H adsorption process. As seen from Figure 8 (d) the regions of high electron densities are expanded from H and Pt sites to Ti sites but they are not symmetric. Furthermore, it can be observed that H

View Article Online
DOI: 10.1039/C6RA12964A

has a greater affinity for Ti atoms than for Pt which is consistent with the OP value of cero for Pt-H (see Table 4).

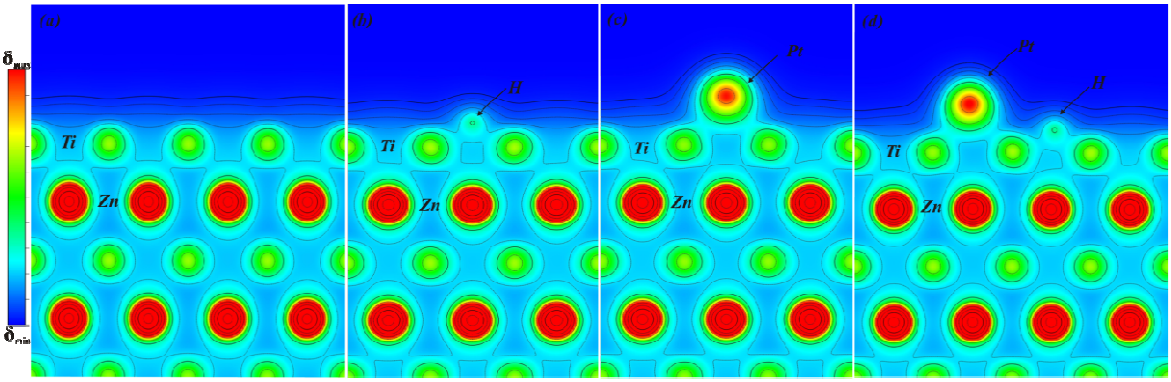

Figure 8. Contour plots of charge density distribution projected along [100] axis of (a) TiZn surface, (b) H-TiZn, (c) Pt-TiZn and (c) H-Pt/TiZn systems. Blue -Green- Red colour scale was used, ranging from red for high to blue for low electron density.

View Article Online
DOI: 10.1039/C6RA12964A

4. CONCLUSIONS

Spin-polarized density functional theory (DFT) calculations were performed in order to understand the interaction among H, Pt and B2-TiZn (001) surface at a microscopic level. It was found that the Pt doping enhances significantly the hydrogen adsorption process on the alloy. This behavior was explained by a throughout analysis of their electronic and chemical bonding properties.

Both H and Pt prefer to be adsorbed on the hollow site where the higher coordination number allows them to minimize the repulsion among the overlapping charge densities of H, Pt and surface. Moreover, $3d_{x^2-y^2}$, $3d_{z^2}$ and $3p_z$ Ti, $5p_z$ Pt orbitals play an important role in this process and the high overlapping among Pt and Ti orbitals enables a more effective H bonding to the surface. This is a result of charge transfer among interacting atoms, H and Pt accept charge density from Ti atoms which constitute the hollow sites. It was also found that the adsorption of H and Pt on the surface changes the total magnetic moment, due to the interaction among H and Pt single spin and open *d* shells of Ti atoms. Finally, it was useful the bonding analysis from SIESTA and DDEC6 being the last a direct application from VASP output data.

View Article Online
DOI: 10.1039/C6RA12964A

ACKNOWLEGEMENT

We acknowledge the financial support given by SGCyT-UNS, CONICET - PIP 2014-2016: GI11220130100436CO, PICT-2012-1609, PICT-2014-1351, Res. 4541/12 and 774/13 as well as Research Council of Norway (YGGDRASIL grant N° 227272/F11). VV, AJ and EG are members of CONICET. We kindly acknowledge useful discussions with Prof. Ricardo Faccio and Dr. Pablo Bechthold. We also thank reviewers for their valuable recommendations.

View Article Online
DOI: 10.1039/C6RA12964A

REFERENCES

1. I. Dincer, Int. J. Hydrogen Energy, 2002, **27**, 265-285.
2. A. Züttel, Mater. Today 2003, **6**, 24-33.
3. H. Smithson, C.A. Marianetti, D. Morgan, A. Van der Ven, A. Predith, G. Ceder, Phys. Rev. B, 2002, **66**, 144107
4. D.G. Ivey, D.O. Northwood, J. Mater. Sci., 1983, **18**, 321–347.
5. S.A. Sherif, F. Barbir, T.N. Veziroglu, Solar Energy, 2005, **78**, 647–660.
6. B. Sakintuna, F Lamari-Darkrim, M. Hirscher, Int. J. Hydrogen Energy, 2007, **32**, 1121-1140.
7. P. Ping Chen, M. Zhu, Mater. Today, 2008, **11**, 36-43.
8. E.C.E. Ronnebro, E.H. Majzoub, MRS Bull., 2013, **38**, 452–458.
9. N. Novaković, J.G. Novaković, L.J. Matović, I. Radisaljević, M. Manasijević, N. Ivanović, Int. J. Hydrogen Energy 2010, **35**, 598–608.
10. C. Zhou, Z.Z. Fang, R. C. Bowman Jr., J. Phys. Chem. C 2015, **119**, 22261–22271.
11. W. Grochala, P.P. Edwards, Chem. Rev. 2004, **104**, 1283–1315.
12. A. Zaluska, L. Zaluski, J.O. Ström-Olsen, J. Alloys Compds., 1999, **288**, 217–225.
13. G. Barkhordarian, T. Klassen, R. Bormann, J. Alloys Compds, 2004, **364**, 242–246.
14. E. David, J. Mater. Process. Technol., 2005, **162-163**, 169–177.
15. P. Corbo, F. Migliardini, O. Veneri, *Hydrogen Fuel Cells for Road Vehicles – Green Energy and Technology*, Springer-Verlag, London, **2011**
16. G.L. Leone, H.W. Kerr, J. Cryst. Growth, 1976, **32**, 111–116
17. G.P. Vassilev, X.J. Liu, K. Ishida, J. Alloys Compd., 2004, **375**, 162-170.
18. G. Ghosh, S. Delsante, G .Borzone, M. Asta, R. Ferro, Acta Mater., 2006, **54**, 4977-4997.
19. T. Ishikawa, M. Murai, K. Kandori, T. Nakayama, Corros. Sci., 2006, **48**, 3172-3185.
20. R.V. Chepulskii, S. Curtarolo, Acta Mater., 2009, **57**, 5314-5323.
21. G. Reumont, T. Gloriant, P. Perrot, J. Mater. Sci. Lett., 1997, **16**, 62-65.
22. A.R. Marder, Prog. Mater. Sci., 2000, **45**, 191-27
23. Y. Gui , Q-Y. Xu, Y-L. Guo, J. Iron Steel Res. Int., 2014, **21**, 396–402
24. T. Tsuru, T. Hirasaki, A. Nishikawa, CAPS-ISIJ., 2003, **15**, 1192–1194
25. S. D. Cramer, B. S. Covino, Jr, *ASM Handbook, Volume 13A, Corrosion: Fundatmentals, Testing, and Protection*, ASM International, New York, **2003**
26. A.R. Marder, Prog. Mater. Sci., 2000, **45**, 191-271
27. F. Li, X. Gao, Q. Xue, S. Li, Y. Che, J.M. Lee, Nanotechnology, 2015, **26**, 065603-1-8
28. Z. Duan, Z. Jun, Zhong, G. Wang, J. Chem. Phys., 2010, **133**, 114701-1-11
29. A. Chen, P. Holt-Hindle, Chem. Rev., 2010, **110**, 3767–3804
30. W. Kohn, L.J. Sham, Phys. Rev., 1965, **140**, A1133-A1138.
31. G. Kresse, J. Furthmuller, Comput. Mater. Sci., 1996, **6**, 15-50.
32. G. Kresse, D. Joubert, Phys. Rev. B; 1999, **59**, 1758-1775.
33. P.E. Blöchl, Phys. Rev. B, 1994, **50**, 17953–17979
34. B. Hammer, L.B. Hansen, J.K. Nørskov, Phys. Rev. B, 1999, **59**, 7413–7421
35. H.J. Monkhorst, J.D. Pack, Phys. Rev. B, 1976, **13**, 5188–5192
36. R.J. Hoffmann, *Solids and Surfaces: A Chemist's View of Bonding in Extended Structures*, VCH, New York, **1988**.
37. R. Dronskowski, *Computational Chemistry of Solid State Materials: A Guide for Materials Scientists, Chemists, Physicists and others*; Wiley-VCH: Weinheimr, **2005**
38. P. Ordejón, E. Artacho, J. M. Soler, Phys. Rev. B: Condens. Matter. Mater. Phys., 1996, **53**, R10441−R10444.
39. J. M. Soler, E. Artacho, J. D. Gale, A. Garcia, J. Junquera, P. Ordejón, D. Sanchez-Portal, J. Phys.: Condens. Matter., 2002, **14,** 2745−2779.
40. S. Pirillo, I. López-Corral, E. Germán, A. Juan, Vacuum, 2014, **99**, 259-264

View Article Online
DOI: 10.1039/C6RA12964A

41. H. Seitz, C. Luna, A. Juan, G. Brizuela, B. Irigoyen, J. Phys. Chem. C 2015, **119**, 4967−4975.
42. S.F. Matar, J. Magn. Magn Mater., 2014, **368**, 105-110
43. G. M. Rangger, L. Romaner, O. T. Hofmann, G. Heimel, M. G. Ramsey, E. Zojer, J. Chem. Theory Comput. 2010, **6**, 3481–3489
44. K. K. Amara, Y.Chen, Y-C. Lin, R. Kumar, E. Okunishi, K. Suenaga, S. Y. Quek, G. Eda, Chem. Mater., 2016, **28**, 2308–2314
45. N. Gabaldon-Limas, T. A. Manz, RSC Adv., 2016, **6**, 45727-45747.
46. T. A. Manz, N. Gabaldon-Limas, RSC Adv., 2016, **6**, 47771-47801.
47. T. A. Manz, N. Gabaldon Limas, Chargemol program for performing DDEC analysis, Version 3.4.4, **2016**, ddec.sourceforge.net
48. R. F. W. Bader, *Atoms in Molecules - A Quantum Theory,* Oxford University Press, Oxford, **1990**
49. W. Tang, E. Sanville, G. Henkelman, J. Phys: Condens. Matter., 2009, **21**, 084204.
50. W. Heine, U. Zwicker, Z. Metallkd, 1962, **53**, 380-385
51. G. Lee, J.S. Kim, Y.M. Koo, S.E. Kulkova, Int. J. Hydrogen Energy, 2002, **27**, 403-412
52. K.P. Huber, G. Hertzberg, *Molecular Spectra and Molecular Structure IV: Constants of Diatomic Molecules,* Van Norstrand Reinhold, New York, **1979**.
53. V. Verdinelli, E. German, C.R..Luna, J.M..Marchetti, M.A. Volpe, A. Juan, J. Phys. Chem. C, 2014, **118**, 27672−27680.
54. R.E. Watson, M. Weinert, Solid State Phys., 2001, **56**, 1-112
55. S.S. Kulkov, S.V. Eremeev, S.E. Kulkova, Phys. Solid State, 2009, **51**,1281-1289
56. G. Kresse, J. Hafner, Surf. Sci., 2000, **459**, 287-302
57. M. Gupta, E. Rodriguez, J. Alloys Compd., 1995, **219**, 6-9
58. V. Celik, H. Unal, E. Mete, S. Ellialtıoglu, Phys. Rev. B , 2010, **82**, 205113_1-205113_12
59. S. Kulkova, D. Chudinov, S. Eremeev, S. Kulkov, Internet Electron. J. Mol. Des., 2004, **3**, 720–727.
60. L. Jeloaica, V. Sidis, Chem. Phys. Lett., 1999, **300**, 157-162.
61. H. Zhuang, A. J. Tkalych, E. A. Carter, J. Electrochem. Soc., 2016, **163** (7), F629-F636
62. J.A. Rodríguez; D.W. Goodman, Science, 1992, **257**, 897-903